Journal of Quantitative Spectroscopy & Radiative Transfer 111 (2010) 2279–2290

Contents lists available at ScienceDirect

Journal of Quantitative Spectroscopy & Radiative Transfer

journal homepage: www.elsevier.com/locate/jqsrt

A theoretical-spectroscopy, *ab initio*-based study of the electronic ground state of $^{121}SbH_3$

Sergei N. Yurchenko [a,*], Miguel Carvajal [b], Andrey Yachmenev [c], Walter Thiel [c], Per Jensen [d]

[a] *Technische Universität Dresden, Institut für Physikalische Chemie und Elektrochemie, D-01062 Dresden, Germany*
[b] *Departamento de Física Aplicada, Facultad de Ciencias Experimentales, Avenida de las Fuerzas Armadas s/n, Universidad de Huelva, E-21071 Huelva, Spain*
[c] *Max-Planck-Institut für Kohlenforschung, Kaiser-Wilhelm-Platz 1, D–45470 Mülheim an der Ruhr, Germany*
[d] *Theoretische Chemie, Bergische Universität, D-42097 Wuppertal, Germany*

ARTICLE INFO

Article history:
Received 22 January 2010
Received in revised form
5 March 2010
Accepted 8 March 2010

Keywords:
Stibine
Rovibrational
Line list
Ab initio
Potential surface
Dipole moment surface

ABSTRACT

For the stibine isotopologue $^{121}SbH_3$, we report improved theoretical calculations of the vibrational energies below 8000 cm^{-1} and simulations of the rovibrational spectrum in the 0–8000 cm^{-1} region. The calculations are based on a refined *ab initio* potential energy surface and on a new dipole moment surface obtained at the coupled cluster CCSD(T) level. The theoretical results are compared with the available experimental data in order to validate the *ab initio* surfaces and the TROVE computational method [Yurchenko SN, Thiel W, Jensen P. J Mol Spectrosc 2007;245:126–40] for calculating rovibrational energies and simulating rovibrational spectra of arbitrary molecules in isolated electronic states. A number of predicted vibrational energies of $^{121}SbH_3$ are provided in order to stimulate new experimental investigations of stibine. The local-mode character of the vibrations in stibine is demonstrated through an analysis of the results in terms of local-mode theory.

1. Introduction

Over a period of several years we have developed theoretical models, of increasingly wider applicability, that describe the rotational and vibrational motion of polyatomic molecules in isolated electronic states. Our initial work was concerned with XY_3 ammonia-type molecules and led to the XY3 theoretical model and computer program for calculating the rotation–vibration energies [1–3], and simulating the rotation–vibration spectra [4–7] for such molecules. The XY3 approach is entirely variational in that the rotation–vibration energies and wavefunctions are obtained by diagonalization of a matrix representation of the rotation–vibration Hamiltonian, constructed in a suitable basis set. The rotation–vibration Hamiltonian employed is based on 'spectroscopic' ideas: Following the theory of Hougen et al. [8], small-amplitude vibrational motion is described in terms of displacements from a reference structure which follows the large-amplitude inversion (umbrella-flipping) motion of an NH_3-type molecule. The XY3 rotation–vibration Hamiltonian is expanded as a power series in the coordinates describing the small-amplitude vibrations.

More recently, we have implemented ideas similar to those of the XY3 approach in the more general program TROVE (Theoretical ROtation–Vibration Energies) [9] which, at least in principle, can calculate the rotation–vibration energies [9], and simulate the rotation–vibration spectra [10], for any molecule in an isolated electronic state. Also in the TROVE model, the rotation–vibration Hamiltonian is expanded as a power series in small-amplitude vibrational coordinates describing vibrational displacements from a reference configuration which can be rigid, as in customary, spectroscopic rotation–vibration theory [11] or flexible as in the Hougen–Bunker–Johns theory [8].

* Corresponding author. Tel.: +49 351 463 33635; fax: +49 351 463 35953.
E-mail address: s.yurchenko@chemie.tu-dresden.de (S.N. Yurchenko).

0022-4073/$ - see front matter © 2010 Elsevier Ltd. All rights reserved.
doi:10.1016/j.jqsrt.2010.03.008

We have applied the XY3 and TROVE programs to a series of XH_3 molecules (X=N,P,As,Sb,Bi) [1,2,5–7,10,12–17]. Also, TROVE has been used to predict and interpret the complicated torsional splittings of the HSOH molecule [18], to explain an intensity anomaly observed in this molecule [19,20] and to predict highly excited rotational energies in deuterated isotopologues of BiH_3, SbH_3, and AsH_3 [21]. The theoretical calculations of rotation–vibration energies and intensities are generally based on *ab initio* potential energy surfaces (PES) and dipole moment surfaces (DMS); in some instances we have refined the analytical representations of the PES in simultaneous least-squares fittings to experimentally derived vibrational energy spacings and *ab initio* data.

Our studies of the various XH_3 molecules (X=N, P, As, Sb, Bi) have had a different emphasis. For NH_3, the potential energy barrier to inversion is easily surmountable and energy splittings resulting from the inversion are readily observable. Thus, in the description of the vibrational motion of NH_3 it is imperative to account correctly for the strongly anharmonic inversion motion. NH_3 is an important molecule in astrophysical and atmospheric contexts and, to facilitate studies in these areas, there is interest in accurate predictions of its rotation–vibration spectra. Thus, our investigations of NH_3 have been generally focused on producing such predictions [1,4,5,13]; this work has culminated in a recent project aimed at the generation of a so-called line list (a database of NH_3 transition wavenumbers and line strengths to be used in astrophysical and atmospheric work) for NH_3 by means of the TROVE program [10]. The remaining molecules in the XH_3 series, PH_3, BiH_3, SbH_3, and AsH_3, are of less astrophysical importance than NH_3 (although PH_3 was observed in Jupiter and Saturn [22] and an intensive search of the interstellar and circumstellar medium is being carried out [23]). They have high potential energy barriers to inversion so that the inversion motion is effectively replaced by a small-amplitude bending motion. These molecules, however, show distinct local mode behavior [17,24,25] and we have predicted theoretically that, in consequence, they exhibit energy-cluster formation at high rotational excitation [6,12,15]. Our theoretical studies of these molecules have been generally aimed at providing predictions for laboratory spectroscopy with the hope of facilitating the experimental characterization of the energy cluster states. In particular, quite recently [21] we have carried out TROVE calculations for singly and di-deuterated isotopologues of PH_3, BiH_3, and SbH_3 (together with some effective-rotational-Hamiltonian calculations for AsH_2D and $AsHD_2$), demonstrating for the first time that some of these isotopologues have energy clusters.

In the present paper, we extend our previous work on stibine SbH_3 [15], in particular by computing values for the electric dipole transition moments based on a new *ab initio* DMS and on a 'spectroscopic' PES that is determined by least-squares fitting to available experimentally derived vibrational energies, using an *ab initio* PES [15,26,27] as starting point. To calculate the *ab initio* DMS we used the CCSD(T) method in conjunction with the pseudopotential ECP46MWB [28] and the SDB-aug-cc-pVTZ basis [29] to describe the Sb atom and the aug-cc-pVTZ basis set [30] to describe the hydrogen atoms. With the new DMS and the refined PES, we have carried out calculations of vibrational and rovibrational states for the $^{121}SbH_3$ isotopologue, and we have simulated the spectrum of this molecule in the wavenumber range 0–8000 cm^{-1}. In order to improve the agreement with experiment of the synthetic absorption spectrum, the empirical basis set correction (EBSC) was utilized [10], in which the vibrational energies were shifted to the experimental values in the rovibrational calculations (see the text below for details). In addition, the energy level pattern resulting from the cluster formation has been qualitatively analyzed in terms of local-mode theory.

The first experimental spectroscopic study of stibine was made in 1951 by Loomis et al. [31] who observed rotational spectra in the vibrational ground state of $^{121}SbH_2D$ and $^{123}SbH_2D$. Later on, microwave spectra were recorded for the ground vibrational states of $^{121}SbH_3$, $^{123}SbH_3$, $^{121}SbD_3$, and $^{123}SbD_3$ [32,33]. In the infrared region, spectra of different vibrational bands for $^{121}SbH_3$ and $^{123}SbH_3$ were subsequently measured and analyzed [34–40]; these works produced experimental values for vibrational term values up to 12 000 cm^{-1} above the vibrational ground state with the largest number of vibrational states being investigated for $^{121}SbH_3$. Halonen et al. [35] reported relative band intensities for stretching vibrational bands with up to four stretching quanta excited. Recently, the high-resolution infrared spectrum of $^{121}SbD_3$ was recorded and various fundamental levels were characterized by Canè et al. [27].

On the theoretical side, Halonen et al. [34,35,37] complemented their experimental studies of stibine by computing vibrational energies by means of local-mode models. Another local mode analysis of the vibrational energies of stibine was carried out by means of the creation and annihilation operators technique [41,42]. *Ab initio* studies [26,27] were performed to calculate the PES, the dipole moments, the equilibrium geometries, and effective rotation–vibration constants for $^{121}SbH_3$ and $^{123}SbH_3$, and $^{123}SbD_3$. Pluchart et al. [43] used their algebraic approach to describe vibrational modes of SbH_3. Liu et al. [44] reported an *ab initio* three-dimensional Sb–H stretching DMS of SbH_3 together with band intensities for stretching bands below 11 000 cm^{-1}.

Even the most recent *ab initio* PESs of stibine computed at state-of-the-art level of theory [27] are not sufficiently accurate for spectroscopic applications. This situation is usually resolved by adjusting the PES empirically in fits to experimental data. A number of 'spectroscopic' PESs of stibine [35,37,41,43] have been obtained by least-squares fitting to the available experimental band centers.

In the present work we report calculations that aim at an improved theoretical description of the vibration–rotation spectrum of stibine. We start from an *ab initio* PES of stibine [27] and refine it by fitting to the available experimental band centers. We also compute a new six-dimensional *ab initio* DMS of SbH_3, which is utilized for simulating the absorption spectrum at an absolute temperature of T=300 K.

The structure of this paper is as follows. In Section 2 we describe the variational procedure used for the nuclear-motion calculations; in Section 3 the refinement of the PES is presented; in Section 4 we report theoretical absorption intensities of $^{121}SbH_3$ (T=300 K); and a local mode analysis is performed in Section 5. In Section 6 we give some conclusions.

2. Computational details of the variational TROVE calculation

We have used the variational program TROVE [9] to calculate the rovibrational energies, eigenfunctions, and matrix elements of the electric dipole moment of $^{121}SbH_3$; these quantities are necessary for the simulation of the absorption spectrum. In the variational calculation, a matrix representation of the rotation–vibration Hamiltonian is diagonalized. This matrix is set up in terms of a symmetry-adapted contracted basis set constructed as follows. We prepare primitive basis functions as products of one-dimensional (1D) vibrational functions $\phi_{n_1}(r_1^\ell)$, $\phi_{n_2}(r_2^\ell)$, $\phi_{n_3}(r_3^\ell)$, $\phi_{n_4}(\alpha_1^\ell)$, $\phi_{n_5}(\alpha_2^\ell)$, and $\phi_{n_6}(\alpha_3^\ell)$. Here n_i are principal quantum numbers and the six coordinates $(r_1^\ell,r_2^\ell,r_3^\ell,\alpha_1^\ell,\alpha_2^\ell,\alpha_3^\ell)$, are linearized versions [45] of the coordinates r_1, r_2, r_3, α_1, α_2, and α_3. The coordinate r_i is the instantaneous value of the internuclear distance Sb–H_i, where H_i is the proton labeled i=1, 2, or 3, whilst the bond angles are given as $\alpha_1=\angle(H_2SbH_3)$, $\alpha_2=\angle(H_1SbH_3)$, and $\alpha_3=\angle(H_1SbH_2)$. Each set of $\phi_{n_i}(q_i)$ functions is obtained by solving, with the Numerov–Cooley technique [46,47], the one-dimensional (1D) Schrödinger equation [9] for the vibrational motion associated with the coordinate $q_i\in\{r_1^\ell,r_2^\ell,r_3^\ell,\alpha_1^\ell,\alpha_2^\ell,\alpha_3^\ell\}$, when the other coordinates are held fixed at their equilibrium values. The 1D functions could also be chosen so that they describe a 1D motion along a minimum energy path with all other coordinates relaxing so as to minimize the potential energy; such 1D functions are generated in the semi-rigid bender (SRB) approach first proposed by Bunker and Landsberg in 1977 [48]. The SRB-generated 1D functions may be slightly better approximations for the true wavefunctions than the 'rigid-bender-type' 1D functions [48] we use here. However, they are more complicated to generate and normally produce only a modest gain in computational efficiency for the total variational calculation. The basis set functions $\phi_{n_i}(q_i)$ are used in a variational solution of the J=0 vibrational problem:

$$\hat{H}_{\rm vib}|\Psi^{\Gamma}_{J=0,\gamma}\rangle=E^{\rm vib}_{\gamma}|\Psi^{\Gamma}_{J=0,\gamma}\rangle, \tag{1}$$

where $\hat{H}_{\rm vib}$ is the vibrational (J=0) Hamiltonian

$$\hat{H}_{\rm vib}=\frac{1}{2}\sum_{\lambda\mu}p_\lambda G_{\lambda\mu}p_\mu+V+U, \tag{2}$$

$E^{\rm vib}_{\gamma}$ and $\Psi^{\Gamma}_{J=0,\gamma}$ are the vibrational eigenvalues and eigenfunctions, respectively, and $\Gamma=A_1,A_2,E$ are the irreducible representations of the $\boldsymbol{C}_{3v}$(M) molecular symmetry group [45] to which SbH_3 belongs. In Eq. (2), p_λ and p_μ are generalized momenta conjugate to the coordinates q_λ and q_μ, respectively. The Hamiltonian $H_{\rm vib}$ is consistent with the volume element $dq_1\,dq_2\,dq_3\,dq_4\,dq_5\,dq_6$. In Eq. (2) the $G_{\lambda\mu}$ are kinetic energy factors (which depend on the vibrational coordinates), U is the pseudopotential, and V is the molecular potential energy function [9]. We use here the type of Hamiltonian where all vibrations are described as displacements from a rigid reference configuration, i.e., the Hamiltonian is given as an expansion around the equilibrium geometry (see below). In this case our $G_{\lambda\mu}$ matrix elements coincide with the Wilson G matrix elements [49]. Since the Hamiltonian is totally symmetric [45] in $\boldsymbol{C}_{3v}$(M), its eigenfunctions $\Psi^{\Gamma}_{J=0,\gamma}$ are automatically symmetrized, i.e., they must necessarily transform according to one of the irreducible representations of $\boldsymbol{C}_{3v}$(M). The details of our approach to recognizing and analyzing the symmetries of the $\Psi^{\Gamma}_{J=0,\gamma}$ functions will be reported elsewhere. In setting up the matrix representations of the rotation–vibration Hamiltonian for $J>0$ we use symmetrized basis functions $\Psi^{\Gamma}_{J,K,\gamma}$ obtained from the products $\Psi^{\Gamma}_{J=0,\gamma}|J,K,m,\tau_{\rm rot}\rangle$, where $|J,K,m,\tau_{\rm rot}\rangle$ is a symmetrized symmetric top rotational eigenfunction [3]. The quantum number $\tau_{\rm rot}$ (=0 or 1) determines the parity of the function [45] (the rotational parity) as $(-1)^{\tau_{\rm rot}}$ and $K\geq 0$ and m (where $-J\leq m\leq J$) are the projections, in units of $\hbar$, of the rotational angular momentum onto the molecule-fixed z-axis and the space-fixed Z-axis, respectively [45]. This basis set will be referred to as a (J=0)-contracted basis set [10].

The (J=0)-contraction offers a number of important advantages. The vibrational part $\hat{H}_{\rm vib}$ of the total Hamiltonian is diagonal in the (J=0)-basis set functions $\Psi^{\Gamma}_{J=0,\gamma}$ and thus its matrix elements are given completely by the eigenvalues $E^{\rm vib}_{\gamma}$ and do not need to be calculated. Another advantage is that for spectrum simulations the theoretical vibrational term values $E^{\rm vib}_{\gamma}$ can be substituted by the available experimental values [10]. This so-called empirical basis set correction (EBSC) scheme was introduced in Ref. [10], where it was used to improve the agreement with experiment for the synthetic spectra. We also employ the EBSC approach in the spectrum simulations of the present work.

In order to define the TROVE Hamiltonian we must define the expansion orders for its kinetic-energy and potential-energy parts. The expansions of $G_{\lambda\mu}$ and U in the coordinates $\{r_1^\ell,\ r_2^\ell,\ r_3^\ell,\ \alpha_1^\ell,\ \alpha_2^\ell,\ \alpha_3^\ell\}$, are truncated after the 6th-order terms while the expansion of V in the coordinates $\{\xi_1^\ell,\ \xi_2^\ell,\ \xi_3^\ell,\ \alpha_1^\ell,\ \alpha_2^\ell,\ \alpha_3^\ell\}$ is truncated after the 8th-order terms. Here $\xi_i^\ell=1-\exp[-a(r_i^\ell-r_e)]$ where a=1.4 Å^{-1} is a Morse parameter and r_e is the equilibrium bond length. In TROVE the size of the basis set, and therefore the size of the Hamiltonian matrix, is controlled by the polyad number defined as

$$P=2(n_1+n_2+n_3)+n_4+n_5+n_6, \tag{3}$$

where the local-mode quantum numbers n_i are defined in connection with the primitive basis functions ϕ_{n_i}. That is, we include in the primitive basis set only those combinations of ϕ_{n_i} for which $P\leq P_{\rm max}$. In present work we use $P_{\rm max}$=12 for the calculations of vibration energies J=0, including those made in connection with the empirical refinement of the PES, and $P_{\rm max}$=10 for the intensity simulations. The smaller $P_{\rm max}$-value used for the simulations helps to make the computation of

Table 1
Experimentally derived vibrational energies of $^{121}SbH_3$ (in cm^{-1}) compared with theoretical values.

State[a]	n_1[b]	n_2	n_3	n_4	n_5	n_6	Γ[c]	Obs.[d]	Calc. I[e]	Calc. II[f]
v_2	0	0	0	1	0	0	A_1	782.245[g]	799.04	782.18
v_4	0	0	0	1	0	0	E	827.855[g]	836.77	827.81
$2v_2$	0	0	0	1	1	0	A_1	1559.0	1594.21	1559.26
$2v_4$	0	0	0	2	0	0	A_1	1652.7	1669.03	1653.63
v_1	1	0	0	0	0	0	A_1	1890.503[g]	1894.24	1890.71
v_3	1	0	0	0	0	0	E	1894.497[g]	1899.65	1894.53
v_1+v_2	1	0	0	1	0	0	A_1	2661	2686.16	2661.61
v_1+v_4	1	0	0	1	0	0	E	2705	2719.80	2706.42
v_1+v_3	2	0	0	0	0	0	E	3719.860	3732.53	3719.67
$2v_3$	2	0	0	0	0	0	A_1	3719.933	3732.51	3719.96
$2v_3+v_4$	2	0	0	1	0	0	E	4513[h]	4541.89	4521.00[i]
$v_1+v_3+v_4$	1	1	0	1	0	0	A_1	4545[h]	4563.44	4539.19[j]
$2v_1+v_3$	3	0	0	0	0	0	E	5480.235	5506.41	5480.40
v_1+2v_3	3	0	0	0	0	0	A_1	5480.285	5506.52	5481.16
–	2	1	0	0	0	0	E	5607[h]	5632.72	5606.10
$3v_1$	2	1	0	0	0	0	A_1	5607[h]	5623.09	5609.20
v_1+3v_3	4	0	0	0	0	0	E	7173.783	7222.65	7178.35
$2v_1+2v_3$	4	0	0	0	0	0	A_1	7173.799	7222.67	7178.45

[a] Spectroscopic assignment of the vibrational state [42] when available.
[b] The local-mode quantum numbers n_i obtained presently as defined by the 1D basis functions ϕ_{n_i} (see text).
[c] Symmetry of the vibrational state in $\boldsymbol{C}_{3v}$(M).
[d] Experimentally derived vibrational term values from Ref. [37] unless otherwise indicated.
[e] Energies calculated with TROVE from the *ab initio* PES of Ref. [15].
[f] Energies calculated with TROVE from the refined PES (see Section 3).
[g] Experimental value from Ref. [40].
[h] Experimental value excluded from the fitting due to its low accuracy.
[i] Another energy with the same-local mode labels is calculated at 4525.70 cm^{-1}; for this state, the intensity of the transition from the vibrational ground state is comparable to that for the state given in the table.
[j] This is the calculated A_1 term value closest to the experimental value. Its local-mode labeling differs from the (2, 0, 0, 1, 0, 0; A_1) assignment in Refs. [37,42]. In the present work, an A_1 term value with this labeling is obtained at 4526.35 cm^{-1} but with a lower intensity for the transition from the vibrational ground state.

highly excited rotational states (with $J \leq 30$) feasible. The largest rotation–vibration matrix block to be diagonalized (J=30, P_{max}=10) had a dimension of 36 720 and was associated with the basis functions of E symmetry.

Recently a full-dimensional variational study of NH_3 based on the exact kinetic energy operator approach was reported by Mátyus et al. [50]. To confirm the consistency of their results with those obtained from the TROVE approach, we recalculated the vibrational term values of NH_3 using the same PES [51] as in Ref. [50] and tight convergence criteria. The basis set and truncation orders of the Hamiltonian were selected in such a way as to guarantee convergence to better than 0.1 cm^{-1}. For the 69 energies below 6000 cm^{-1} reported in Table V of Ref. [50] the root-mean-square (rms) deviation is 0.16 cm^{-1} with the largest deviation of 0.7 cm^{-1} for v_2+3v_4 at 5672.94 cm^{-1}[50].

In the case of SbH_3, we have checked that the effect of truncating the potential energy function (at 8th-order) is <1 cm^{-1} for all vibrational term values below 8000 cm^{-1} and <0.05 cm^{-1} for the values in Table 1. These deviations are significantly smaller than the deviations introduced by the inaccuracy of *ab initio* PES of SbH_3 used presently. The truncation of the kinetic energy operator (at 6th order) affects the vibrational term values by <0.01 cm^{-1}.

3. Refinement of the *ab initio* potential energy surface

As starting point for the SbH_3 calculations of the present work we use the high-level *ab initio* PES by Breidung and Thiel, reported in the paper by Canè et al. [27]. Originally, this PES was given as a standard force constant expansion in terms of the symmetry-adapted coordinates [27]. In connection with recent XY3 calculations aimed at investigating the energy-cluster formation in SbH_3 [15], it was transformed to the expansion [3]

$$V(\xi_1,\xi_2,\xi_3,\xi_{4a},\xi_{4b};\sin\overline{\rho}) = V_e + V_0(\sin\overline{\rho}) + \sum_j F_j(\sin\overline{\rho})\xi_j + \sum_{j\leq k} F_{jk}(\sin\overline{\rho})\xi_j\xi_k + \sum_{j\leq k\leq l} F_{jkl}(\sin\overline{\rho})\xi_j\xi_k\xi_l + \sum_{j\leq k\leq l\leq m} F_{jklm}(\sin\overline{\rho})\xi_j\xi_k\xi_l\xi_m \quad (4)$$

in the coordinates ξ_k:

$$\xi_k = 1-\exp(-a(r_k-r_e)), \quad k=1,2,3, \quad (5)$$

$$\xi_{4a} = \frac{1}{\sqrt{6}}(2\alpha_1-\alpha_2-\alpha_3), \quad (6)$$

$$\xi_{4b} = \frac{1}{\sqrt{2}}(\alpha_2-\alpha_3), \quad (7)$$

$$\sin\overline{\rho} = \frac{2}{\sqrt{3}}\sin[(\alpha_1+\alpha_2+\alpha_3)/6], \quad (8)$$

where

$$V_0(\sin\overline{\rho}) = \sum_{s=1} f_0^{(s)}(\sin\rho_e - \sin\overline{\rho})^s \quad (9)$$

and

$$F_{jk\ldots}(\sin\overline{\rho}) = \sum_{s=0} f_{jk\ldots}^{(s)}(\sin\rho_e - \sin\overline{\rho})^s. \quad (10)$$

We also use this latter expansion in the present work.

In Table 1 we include the available, experimentally derived vibrational term values for $^{121}SbH_3$ (the column labeled 'Obs.') up to 8000 cm^{-1}. The table uses two labeling schemes for the molecular states, one based on the standard normal-mode, harmonic-oscillator quantum numbers and the other one based on local mode, Morse-oscillator quantum numbers [37,41,42]. Lemus et al. [41,42] demonstrated that the bending vibrations in stibine are predominantly of normal mode character, whereas the stretching vibrations are most appropriately described by local mode quantum numbers.

The *ab initio* PES, when used as input for TROVE, produces vibrational energies in rather modest agreement with the available experimental values as seen by comparing the columns labeled 'Obs.' and 'Calc. I' in Table 1. Thus, for the fundamental term values, deviations up to 17 cm^{-1} are found. This accuracy is too poor for most applications. We can improve the agreement with experiment by constructing a 'spectroscopic' PES. Towards this end, we refine the *ab initio* potential parameters [15] of SbH_3 in simultaneous least-squares fitting [2,14] to the available experimentally derived vibrational energy spacings [37,40] and to the *ab initio* data [26]. The fitting employs TROVE calculations of vibrational energies made with the P_{max} = 12 basis set. Following Lummila et al. [37] we discard from the fitting some experimentally derived vibrational energy spacings with high uncertainty (Table 1). Obviously, there are quite few experimentally derived vibrational energy spacings of acceptable accuracy and because of this, a fitting only to these data points would allow the determination of very few potential energy parameter values only. In practice, however, we have been able to obtain values for all relevant potential energy parameters by fitting not only to the experimentally derived vibrational term values but also to the *ab initio* data [26]. In the final fitting to 6455 *ab initio* energies and 14 experimental band center values we could usefully vary 48 potential energy parameters whose optimized values are given in Table 2. During the fitting, the *ab initio* data serve to define the potential energy function in coordinate regions not sampled by the wavefunctions of the experimentally characterized vibrational states.

The vibrational term values calculated with TROVE from the refined, spectroscopic PES are included in Table 1 (Column 'Calc. II') and can be compared with the experimental values. The rms error is 1.83 cm^{-1} for the 14 band centers in the table used in the fittings (0.59 for the term values below 7000 cm^{-1}). The improvement of the calculated vibrational term values of Calc. II with respect to the values of Calc. I is obvious. The local-mode labeling of the calculated states agrees with those given in Refs. [37,41,42] except for the experimental vibrational

Table 2
Parameters (in cm^{-1} unless otherwise indicated) defining the refined PES of SbH_3 in its electronic ground state.

Parameter	Value	Parameter	Value
r_e (Å)	1.700[a]	$f^{(1)}_{114}$	0.11898218331384 $\times 10^6$
α_e (deg)	91.557[a]	$f^{(0)}_{123}$	0.19017877159862 $\times 10^4$
a ($Å^{-1}$)	1.4[a]	$f^{(1)}_{123}$	−0.81887048961300 $\times 10^4$
$f^{(2)}$	0.26647619271542 $\times 10^6$	$f^{(0)}_{124}$	0.12617901283266 $\times 10^4$
$f^{(3)}$	−0.66702427305419 $\times 10^6$	$f^{(1)}_{124}$	0.12728050074026 $\times 10^4$
$f^{(4)}$	0.20692955884057 $\times 10^7$	$f^{(0)}_{144}$	−0.27263329498616 $\times 10^4$
$f^{(1)}_1$	−0.88777775084702 $\times 10^4$	$f^{(1)}_{144}$	−0.41042673137233 $\times 10^5$
$f^{(2)}_1$	−0.17244226542584 $\times 10^5$	$f^{(0)}_{155}$	−0.46758119412010 $\times 10^4$
$f^{(3)}_1$	−0.77196630858319 $\times 10^5$	$f^{(1)}_{155}$	−0.84171112194568 $\times 10^4$
$f^{(0)}_{11}$	0.29586000262748 $\times 10^5$	$f^{(0)}_{455}$	−0.69252855936919 $\times 10^4$
$f^{(1)}_{11}$	0.24713933006405 $\times 10^4$	$f^{(1)}_{455}$	−0.11306727106534 $\times 10^6$
$f^{(2)}_{11}$	−0.75317802775475 $\times 10^5$	$f^{(0)}_{1111}$	0.17507628819530 $\times 10^4$
$f^{(0)}_{12}$	−0.49400706456696 $\times 10^3$	$f^{(0)}_{1112}$	0.41596255026285 $\times 10^4$
$f^{(1)}_{12}$	0.48463297350027 $\times 10^4$	$f^{(0)}_{1114}$	0.10862778013817 $\times 10^5$
$f^{(2)}_{12}$	−0.21107725715571 $\times 10^5$	$f^{(0)}_{1122}$	0.13755090105555 $\times 10^4$
$f^{(0)}_{14}$	−0.10286969463684 $\times 10^4$	$f^{(0)}_{1123}$	−0.93872506047505 $\times 10^4$
$f^{(1)}_{14}$	−0.19498125653409 $\times 10^5$	$f^{(0)}_{1124}$	0.53668552250068 $\times 10^4$
$f^{(2)}_{14}$	0.79078897736870 $\times 10^5$	$f^{(0)}_{1125}$	−0.44737220254204 $\times 10^4$
$f^{(0)}_{44}$	0.15469244272597 $\times 10^5$	$f^{(0)}_{1144}$	−0.10723417778062 $\times 10^5$
$f^{(1)}_{44}$	0.34735788204833 $\times 10^5$	$f^{(0)}_{1155}$	−0.41428780667331 $\times 10^4$
$f^{(2)}_{44}$	−0.20464860777176 $\times 10^6$	$f^{(0)}_{1244}$	0.48983922855174 $\times 10^4$
$f^{(0)}_{111}$	−0.18866575310495 $\times 10^4$	$f^{(0)}_{1255}$	0.26202447614447 $\times 10^4$
$f^{(1)}_{111}$	−0.39885807692562 $\times 10^5$	$f^{(0)}_{1444}$	0.77940392092530 $\times 10^3$
$f^{(0)}_{112}$	0.42783722357650 $\times 10^2$	$f^{(0)}_{1455}$	−0.23334765139599 $\times 10^4$
$f^{(1)}_{112}$	0.29682625311639 $\times 10^5$	$f^{(0)}_{4444}$	0.30662189381386 $\times 10^4$
$f^{(0)}_{114}$	0.26089106317080 $\times 10^4$		

[a] Fixed in the least-squares fitting to the experimental values from Ref. [38].

Table 3
Experimentally derived rotational term values of $^{121}SbH_3$ in the ground vibrational state (in cm^{-1}) compared to the TROVE-calculated theoretical values.

Γ	J	K	τ_{rot}	Obs.	Calc.	Obs. − Calc.
A_1	0	0	0	0.000	0.000	0.000
E	1	1	0	5.725	5.724	0.002
A_2	1	0	1	5.873	5.868	0.005
E	2	2	0	17.027	17.025	0.002
E	2	1	0	17.470	17.459	0.012
A_1	2	0	0	17.618	17.603	0.015
A_2	3	3	1	33.903	33.903	0.001
A_1	3	3	0	33.903	33.903	0.001
E	3	2	0	34.642	34.626	0.017
E	3	1	0	35.084	35.058	0.026
A_2	3	0	1	35.231	35.202	0.029
E	4	4	0	56.350	56.352	−0.002
A_1	4	3	0	57.386	57.366	0.020
A_2	4	3	1	57.386	57.366	0.020
E	4	2	0	58.122	58.086	0.036
E	4	1	0	58.562	58.516	0.046
A_1	4	0	0	58.708	58.659	0.049
E	5	5	0	84.362	84.368	−0.006
E	5	4	0	85.698	85.675	0.022
A_2	5	3	1	86.729	86.684	0.045
A_1	5	3	0	86.729	86.684	0.045
E	5	2	0	87.461	87.400	0.061
E	5	1	0	87.898	87.828	0.070
A_2	5	0	1	88.044	87.970	0.074
A_1	6	6	0	117.932	117.944	−0.012
A_2	6	6	1	117.932	117.944	−0.012
E	6	5	0	119.571	119.548	0.023
E	6	4	0	120.899	120.847	0.052
A_1	6	3	0	121.923	121.849	0.074
A_2	6	3	1	121.923	121.849	0.074
E	6	2	0	122.650	122.560	0.090
E	6	1	0	123.085	122.985	0.100
A_1	6	0	0	123.229	123.126	0.103

energy of 4545 cm^{-1}. Following Lummila et al. [37] we include neither this level nor the level at 4513 cm^{-1} in the input for the fitting because of the uncertainties of the corresponding term values. In the spectral region around 4500 cm^{-1} there is a high density of vibrational states and so we 'assigned' the two uncertain levels to the theoretically calculated levels that are closest in energy and give rise to strong vibrational transitions from the vibrational ground state, the strength of these transitions being obtained from theoretically calculated intensities (see below).

It should be noted that the correct determination of the molecular equilibrium structure is of special importance for accurate spectrum simulations [10]. In the case of the rigid molecule SbH_3 it is fortunate that the experimental values [38] for the bond length r_e=1.70001 Å and the bond angle $\alpha_e = 91.5566^\circ$ are highly accurate. This is illustrated in Table 3, where we show the theoretical (TROVE) rotational term values of $^{121}SbH_3$ in its ground vibrational state compared to experiment. The corresponding 'experimental' term values were calculated with a Watsonian-type Hamiltonian (see Ref. [45, Section 13.2.4]) in conjunction with the spectroscopic constants reported by Harder et al. [39] without taking into account the hyperfine structure.

4. Electric dipole transition moments and intensities

As a prerequisite for the intensity simulations we have computed the *ab initio* dipole moment surface for SbH_3 employing CCSD(T) (coupled cluster theory with single and double excitations [52] augmented by a perturbational estimate of the effects of connected triple excitations [53]) as implemented in MOLPRO2002 [54,55]. We employed a level of *ab initio* theory similar to that of Ref. [27]. We used a large-core pseudopotential [28] (ECP46MWB) adjusted to quasi-relativistic Wood–Boring [56] all-electron energies to describe the Sb atom in conjunction with the SDB-aug-cc-pVTZ basis [29]. For the hydrogen atoms, we used the aug-cc-pVTZ basis set [30]. In order to account for core–valence correlation effects, the ECP46MWB pseudopotential was supplemented by a core-polarization potential (CPP) in the present CCSD(T) calculations (see also the discussion in Ref. [27]). Dipole moments were computed by a numerical finite-difference procedure with an added external dipole field of 0.001 a.u.

We initially use the *ab initio* dipole moment data to generate an analytical representation of the DMS. For this, we employ the molecular bond (MB) representation [4,5,57,58] as defined in Eq. (35) of Yurchenko et al. [4]. The MB representation is based on the dipole moment projections $(\overline{\boldsymbol{\mu}} \cdot \mathbf{e}_j)$ (where $\mathbf{e}_j$ is a unit vector directed along the Sb–H_j bond and pointing from Sb towards H_j) onto the bonds of the molecule. It defines the DMS completely in terms of the instantaneous positions of the nuclei [4]. The three projections $(\overline{\boldsymbol{\mu}} \cdot \mathbf{e}_j)$ are then expressed in terms of a single function $\overline{\mu}_0(r_1,r_2,r_3,\alpha_1,\alpha_2,\alpha_3)$ [4]:

$$\overline{\boldsymbol{\mu}} \cdot \mathbf{e}_1 = \overline{\mu}_0(r_1,r_2,r_3,\alpha_1,\alpha_2,\alpha_3) = \overline{\mu}_0(r_1,r_3,r_2,\alpha_1,\alpha_3,\alpha_2), \quad (11)$$

$$\overline{\boldsymbol{\mu}} \cdot \mathbf{e}_2 = \overline{\mu}_0(r_2,r_3,r_1,\alpha_2,\alpha_3,\alpha_1) = \overline{\mu}_0(r_2,r_1,r_3,\alpha_2,\alpha_1,\alpha_3), \quad (12)$$

$$\overline{\boldsymbol{\mu}} \cdot \mathbf{e}_3 = \overline{\mu}_0(r_3,r_1,r_2,\alpha_3,\alpha_1,\alpha_2) = \overline{\mu}_0(r_3,r_2,r_1,\alpha_3,\alpha_2,\alpha_1), \quad (13)$$

which is given by the expansion

$$\overline{\mu}_0 = \mu_0^{(0)} + \sum_k \mu_k^{(0)} \chi_k + \sum_{k,l} \mu_{kl}^{(0)} \chi_k \chi_l + \sum_{k,l,m} \mu_{klm}^{(0)} \chi_k \chi_l \chi_m + \sum_{k,l,m,n} \mu_{klmn}^{(0)} \chi_k \chi_l \chi_m \chi_n + \cdots \quad (14)$$

in the variables

$$\chi_k = (r_k - r_e)\exp(-\beta(r_k - r_e)^2), \quad k = 1,2,3, \quad (15)$$

$$\chi_l = \cos(\alpha_{l-3}) - \cos(\alpha_e), \quad l = 4,5,6. \quad (16)$$

In Table 4 the dipole moment parameters for the electronic ground state of SbH_3 are listed. Fitting Eq. (14) through 3×5000 *ab initio* data points, we obtained an rms error of 0.001 D by varying 112 parameters. Fortran routines for calculating the dipole moment components are provided as supplementary material. The new *ab initio* dipole moment function will be referred to as SDB-TZ.

Once the components of the electronically averaged dipole moment $\overline{\mu}_\alpha$ $(\alpha = x,y,z)$ along the molecule-fixed axes *xyz* [3,9] are expressed as functions of the internal molecular coordinates, the matrix elements of the dipole moment components between the molecular eigenfunctions can be obtained. For intensity simulations of the

Table 4
The MB-representation dipole moment parameters [4,5] (in D unless otherwise indicated) for the electronic ground state of stibine.

Parameter	Value	Parameter	Value	Parameter	Value
β (Å^{-1})	1.0	$\mu^{(0)}_{246}$	0.09446641	$\mu^{(0)}_{1566}$	−0.18969200
$\mu^{(0)}_{0}$	−0.15382957	$\mu^{(0)}_{255}$	−0.08714483	$\mu^{(0)}_{1666}$	−0.27524468
$\mu^{(0)}_{1}$	−1.83611199	$\mu^{(0)}_{256}$	−0.12716119	$\mu^{(0)}_{2222}$	0.12706772
$\mu^{(0)}_{3}$	0.12683050	$\mu^{(0)}_{266}$	−0.12409425	$\mu^{(0)}_{2224}$	−0.11429074
$\mu^{(0)}_{4}$	0.09654568	$\mu^{(0)}_{333}$	0.04312205	$\mu^{(0)}_{2225}$	−0.09714754
$\mu^{(0)}_{5}$	−0.86510997	$\mu^{(0)}_{334}$	0.02113440	$\mu^{(0)}_{2244}$	−0.05649518
$\mu^{(0)}_{11}$	0.01993394	$\mu^{(0)}_{344}$	0.04912492	$\mu^{(0)}_{2245}$	−0.11936999
$\mu^{(0)}_{13}$	−0.04946879	$\mu^{(0)}_{444}$	0.06483608	$\mu^{(0)}_{2246}$	0.35605098
$\mu^{(0)}_{14}$	−0.14614088	$\mu^{(0)}_{445}$	0.45316260	$\mu^{(0)}_{2255}$	0.03419155
$\mu^{(0)}_{16}$	0.11984798	$\mu^{(0)}_{456}$	0.01943499	$\mu^{(0)}_{2256}$	−0.05172147
$\mu^{(0)}_{23}$	−0.04886949	$\mu^{(0)}_{466}$	0.08195234	$\mu^{(0)}_{2266}$	0.13911824
$\mu^{(0)}_{33}$	0.04278221	$\mu^{(0)}_{555}$	0.60263858	$\mu^{(0)}_{2333}$	−0.08426329
$\mu^{(0)}_{34}$	−0.12897179	$\mu^{(0)}_{556}$	0.17992418	$\mu^{(0)}_{2335}$	0.06212090
$\mu^{(0)}_{35}$	−0.72509985	$\mu^{(0)}_{1111}$	−0.38455475	$\mu^{(0)}_{2336}$	0.15794728
$\mu^{(0)}_{36}$	0.01665824	$\mu^{(0)}_{1112}$	0.06007596	$\mu^{(0)}_{2344}$	−0.07928812
$\mu^{(0)}_{44}$	−0.03760912	$\mu^{(0)}_{1114}$	−0.07969284	$\mu^{(0)}_{2345}$	0.23880925
$\mu^{(0)}_{46}$	−0.23400948	$\mu^{(0)}_{1115}$	0.35892869	$\mu^{(0)}_{2356}$	0.05479589
$\mu^{(0)}_{55}$	−0.02572926	$\mu^{(0)}_{1122}$	0.15639528	$\mu^{(0)}_{2366}$	0.03429291
$\mu^{(0)}_{56}$	0.09634099	$\mu^{(0)}_{1123}$	0.17820339	$\mu^{(0)}_{2444}$	−0.11772983
$\mu^{(0)}_{111}$	−1.43934622	$\mu^{(0)}_{1124}$	0.09074178	$\mu^{(0)}_{2445}$	−0.34369373
$\mu^{(0)}_{112}$	0.01202344	$\mu^{(0)}_{1126}$	−0.59561584	$\mu^{(0)}_{2456}$	0.33363574
$\mu^{(0)}_{114}$	0.05190559	$\mu^{(0)}_{1136}$	0.20513772	$\mu^{(0)}_{2466}$	0.29436052
$\mu^{(0)}_{115}$	0.51646355	$\mu^{(0)}_{1144}$	−0.03941277	$\mu^{(0)}_{3335}$	−0.54460774
$\mu^{(0)}_{123}$	−0.05792208	$\mu^{(0)}_{1146}$	−0.10634235	$\mu^{(0)}_{3445}$	0.02525874
$\mu^{(0)}_{124}$	0.14067552	$\mu^{(0)}_{1155}$	−0.08258537	$\mu^{(0)}_{3555}$	0.07766749
$\mu^{(0)}_{133}$	0.20671970	$\mu^{(0)}_{1233}$	−0.04666002	$\mu^{(0)}_{3556}$	0.15261861
$\mu^{(0)}_{135}$	0.23858808	$\mu^{(0)}_{1234}$	−0.06445876	$\mu^{(0)}_{3566}$	−0.01376070
$\mu^{(0)}_{136}$	0.01874878	$\mu^{(0)}_{1244}$	−0.13776673	$\mu^{(0)}_{3666}$	−0.04499354
$\mu^{(0)}_{144}$	0.18603743	$\mu^{(0)}_{1245}$	−0.05084070	$\mu^{(0)}_{4444}$	−0.04633795
$\mu^{(0)}_{146}$	0.23528044	$\mu^{(0)}_{1246}$	−0.18584935	$\mu^{(0)}_{4445}$	−0.04439568
$\mu^{(0)}_{155}$	0.67563925	$\mu^{(0)}_{1256}$	−0.26342756	$\mu^{(0)}_{4456}$	−0.40942554
$\mu^{(0)}_{156}$	0.44912683	$\mu^{(0)}_{1335}$	−0.14241433	$\mu^{(0)}_{4466}$	−0.12883163
$\mu^{(0)}_{223}$	0.01144244	$\mu^{(0)}_{1355}$	0.14154362	$\mu^{(0)}_{4555}$	−0.13254513
$\mu^{(0)}_{225}$	0.08900180	$\mu^{(0)}_{1366}$	−0.01688911	$\mu^{(0)}_{4556}$	−0.86386717
$\mu^{(0)}_{226}$	−0.18751441	$\mu^{(0)}_{1444}$	−0.10020889	$\mu^{(0)}_{5566}$	−0.01824977
$\mu^{(0)}_{234}$	0.11085087	$\mu^{(0)}_{1445}$	−0.25372629	$\mu^{(0)}_{5666}$	−0.02576928
$\mu^{(0)}_{235}$	0.04530505	$\mu^{(0)}_{1456}$	−1.32925498	$\mu^{(0)}_{6666}$	0.27677620
$\mu^{(0)}_{245}$	0.43081293	$\mu^{(0)}_{1466}$	−0.28429770		

[a] α_e and r_e were fixed in the least-squares fitting to the *ab initio* [27] equilibrium values of 91.76° and 1.702 Å, respectively.

absorption spectrum of $^{121}SbH_3$ we use the 'spectroscopic' PES and the *ab initio* SDB-TZ DMS in conjunction with the theory described by Yurchenko et al. [4]. We follow the procedures described in Ref. [4] and compute the line strengths (in units of D^2), and the integrated absorption coefficients (in units of cm/mol) for individual rotation–vibration transitions of $^{121}SbH_3$ at T=300 K. In the intensity simulations we considered all transitions within the wavenumber window 0…8000 cm^{-1} with lower states having term values <4000 cm above the ground state. It should be noted that the upper simulation limit (8000 cm^{-1}) is beyond the range in which our PES is optimized (to 7000 cm^{-1}). We have obtained 3 286 305 lines with absorption intensity $I(f\leftarrow i)>0.001$ cm/mol [corresponding to 4×10^{-8} cm^{-2} atm^{-1}] at T=300 K. The eigenfunctions and eigenvalues required for the spectrum simulations were computed with the P_{max}=10 basis set. The EBSC [10] approach was used in order to improve empirically the agreement with experiment of the theoretical spectrum, in which we substituted the theoretical vibrational band centers E^{vib}_{γ} in Eq. (1) by the corresponding experimental values. For more details on the intensity calculations see Ref. [10].

For the calculation of the integrated absorption coefficients $I(f\leftarrow i)$ (see Ref. [4, Eq. (6)]) we require the partition function Q given by [45]

$$Q=\sum_i g_{ns}(2J+1)e^{-E_i hc/kT}, \quad (17)$$

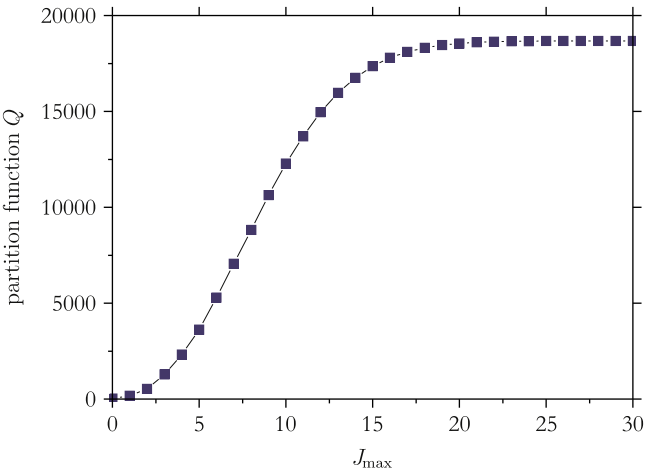

Fig. 1. The convergence of the partition function Q of $^{121}SbH_3$ with $J \le J_{max}$; Q is calculated from all rovibrational states with $P \le P_{max} = 10$ at T=300 K.

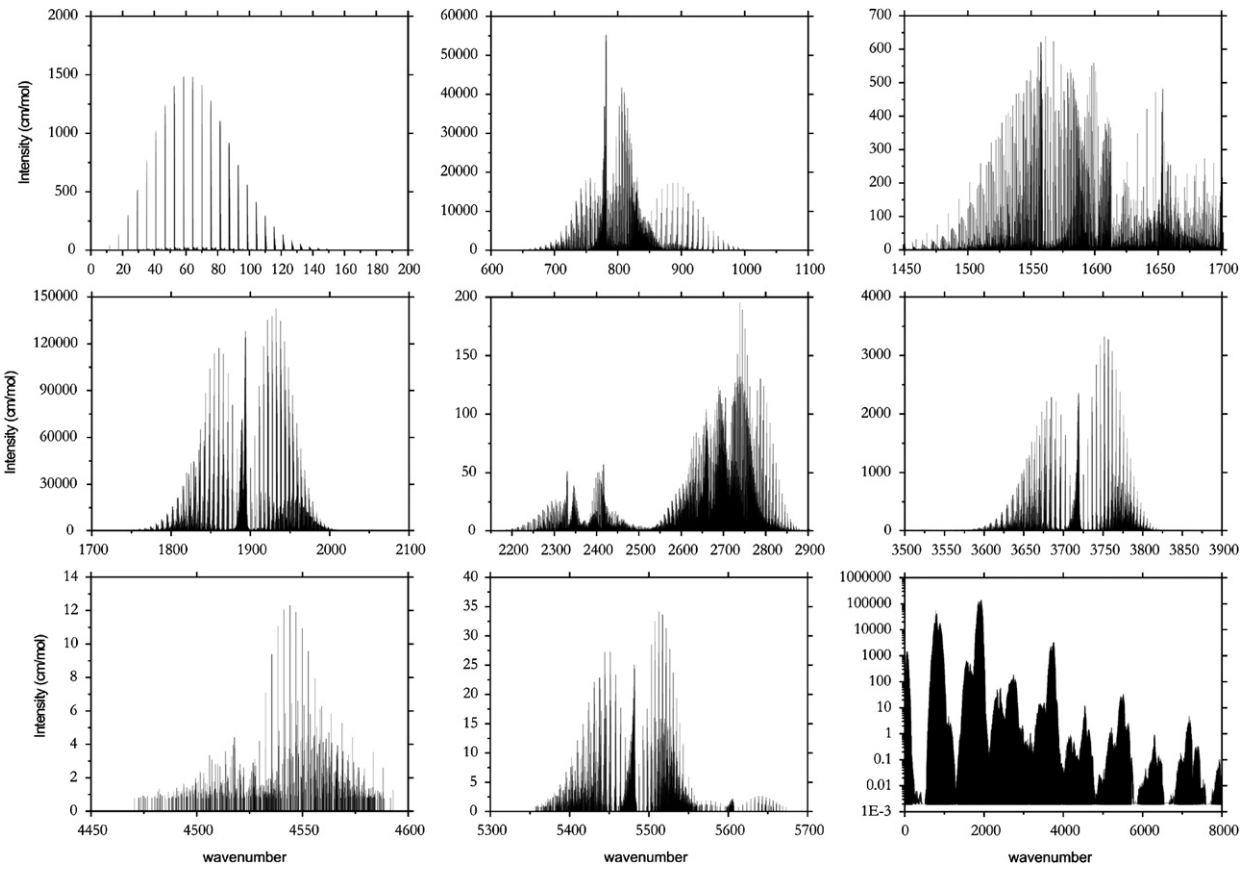

Fig. 2. Synthetic spectra of $^{121}SbH_3$ in the wavenumber range 0–8000 cm^{-1}, computed at an absolute temperature of 300 K.

where g_{ns} is the nuclear spin statistical weight, E_i is a rovibrational term value obtained through diagonalization of the Hamiltonian matrix, k is the Boltzmann constant, h is the Planck constant and c is the speed of light. For the $^{121}SbH_3$ molecule with the nuclear spins of 5/2 and 1/2 for ^{121}Sb and H, respectively, the statistical weight factors g_{ns} for all three symmetries A_1, A_2, and E [45] of $\boldsymbol{C}_{3v}(M)$ are equal to 24. Using all computed rovibrational term values with $J \le 30$ (below 13 657 cm^{-1}, 442 998 levels) in Eq. (17), we obtained Q=18 702. The $^{121}SbH_3$ molecule is an oblate symmetric top with two rotational constants B and C. In the vibrational ground state, these constants have the values 2.937 and 2.789 cm^{-1}, respectively [38], and so we have

Table 5
Vibrational band centers $\tilde{\nu}_{fi}$ (in cm^{-1}), transition moments μ_{fi} (in D), and vibrational band strengths $S_{vib}(f \leftarrow i)$ (Eq. (19) in $cm^{-2}\,atm^{-1}$ at T=300 K) for a number of $^{121}SbH_3$ transitions.

Transition[a]		$\tilde{\nu}_{fi}$	E_f	E_i	μ_{fi}	$S_{vib}(f \leftarrow i)$
Upper state	Lower state					
(000;000;A_1)	(000;000;A_1)	0.00	0.00	0.00	0.331	1.119[b]
(000;120;E)	(000;110;E)	765.23	2422.29	1657.06	0.256	0.021
(000;300;E)	(000;002;E)	766.25	2366.89	1600.64	0.354	0.053
(000;111;A_1)	(000;011;A_1)	772.26	2331.52	1559.26	0.305	0.048
(000;002;E)	(000;001;E)	772.83	1600.64	827.81	0.257	1.147
(000;011;A_1)	(000;001;A_1)	777.08	1559.26	782.18	0.255	1.409
(000;001;A_1)	(000;000;A_1)	782.18	782.18	0.00	0.184	31.534
(000;002;E)	(000;001;A_1)	818.46	1600.64	782.18	0.137	0.431
(000;002;A_1)	(000;001;E)	825.82	1653.63	827.81	0.136	0.346
(000;001;E)	(000;000;A_1)	827.81	827.81	0.00	0.141	19.593
(000;110;E)	(000;001;E)	829.25	1657.06	827.81	0.198	0.733
(000;002;A_1)	(000;001;A_1)	871.45	1653.63	782.18	0.031	0.023
(000;111;A_1)	(000;001;A_1)	1549.34	2331.52	782.18	0.021	0.020
(000;011;A_1)	(000;000;A_1)	1559.26	1559.26	0.00	0.014	0.356
(000;300;E)	(000;001;A_1)	1584.71	2366.89	782.18	0.025	0.029
(000;120;E)	(000;001;E)	1594.48	2422.29	827.81	0.025	0.024
(000;002;E)	(000;000;A_1)	1600.64	1600.64	0.00	0.018	0.618
(000;210;E)	(000;001;E)	1652.79	2480.60	827.81	0.025	0.024
(000;002;A_1)	(000;000;A_1)	1653.63	1653.63	0.00	0.012	0.281
(000;110;E)	(000;000;A_1)	1657.06	1657.06	0.00	0.008	0.134
(100;001;A_1)	(000;001;E)	1833.80	2661.61	827.81	0.041	0.071
(100;001;E)	(000;001;E)	1836.38	2664.19	827.81	0.051	0.112
(100;110;A_2)	(000;110;E)	1862.20	3519.26	1657.06	0.175	0.025
(100;002;E)	(000;002;A_1)	1863.50	3517.13	1653.63	0.221	0.040
(100;110;E)	(000;110;E)	1865.93	3522.99	1657.06	0.224	0.040
(100;011;A_1)	(000;011;A_1)	1866.13	3425.38	1559.26	0.130	0.022
(100;002;A_1)	(000;002;E)	1866.17	3466.81	1600.64	0.158	0.026
(100;011;E)	(000;011;A_1)	1867.73	3426.98	1559.26	0.231	0.069
(100;002;E)	(000;002;E)	1868.43	3469.07	1600.64	0.231	0.057
(100;002;E)	(000;002;E)	1870.58	3471.22	1600.64	0.195	0.040
(100;110;E)	(000;110;E)	1871.73	3528.79	1657.06	0.204	0.034
(100;002;A_2)	(000;002;E)	1871.83	3472.47	1600.64	0.175	0.032
(100;001;E)	(000;001;E)	1878.61	2706.42	827.81	0.239	2.470
(100;001;A_1)	(000;001;E)	1878.68	2706.49	827.81	0.173	1.296
(100;001;A_1)	(000;001;A_1)	1879.43	2661.61	782.18	0.140	1.055
(100;001;A_2)	(000;001;E)	1881.52	2709.33	827.81	0.178	1.377
(100;001;E)	(000;001;E)	1881.86	2709.67	827.81	0.214	1.992
(100;001;E)	(000;001;A_1)	1882.01	2664.19	782.18	0.244	3.223
(100;000;A_1)	(000;000;A_1)	1890.71	1890.71	0.00	0.146	48.931
(100;000;E)	(000;000;A_1)	1894.53	1894.53	0.00	0.251	146.160
(100;001;A_1)	(000;001;A_1)	1924.31	2706.49	782.18	0.031	0.054
(100;001;E)	(000;001;A_1)	1927.50	2709.67	782.18	0.053	0.155
(000;111;A_1)	(000;000;A_1)	2331.52	2331.52	0.00	0.004	0.042
(000;111;A_1)	(000;000;A_1)	2417.89	2417.89	0.00	0.004	0.039
(100;001;A_1)	(000;000;A_1)	2661.61	2661.61	0.00	0.005	0.079
(100;001;E)	(000;000;A_1)	2664.19	2664.19	0.00	0.006	0.127
(100;001;E)	(000;000;A_1)	2706.42	2706.42	0.00	0.007	0.173
(100;001;A_1)	(000;000;A_1)	2706.49	2706.49	0.00	0.005	0.082
(100;001;E)	(000;000;A_1)	2709.67	2709.67	0.00	0.003	0.031
(100;002;E)	(000;000;A_1)	3471.22	3471.22	0.00	0.002	0.024
(200;001;E)	(000;001;A_1)	3690.29	4472.46	782.18	0.023	0.058
(020;001;A_1)	(000;001;A_1)	3690.36	4472.54	782.18	0.015	0.024
(200;001;A_2)	(000;001;E)	3692.60	4520.41	827.81	0.018	0.029
(200;001;E)	000;001;E)	3693.19	4521.00	827.81	0.025	0.053
(020;001;E)	(000;001;E)	3697.89	4525.70	827.81	0.022	0.043
(200;001;A_1)	(000;001;E)	3698.54	4526.35	827.81	0.017	0.023
(200;000;E)	(000;000;A_1)	3719.67	3719.67	0.00	0.026	3.022
(020;000;A_1)	(000;000;A_1)	3719.96	3719.96	0.00	0.017	1.270
(110;000;E)	(000;000;A_1)	3794.30	3794.30	0.00	0.002	0.021
(300;000;E)	(000;000;A_1)	5480.40	5480.40	0.00	0.002	0.029
(003;000;A_1)	(000;000;A_1)	5481.16	5481.16	0.00	0.002	0.026

The threshold for the vibrational line strengths was taken to be 0.02 $cm^{-2}\,atm^{-1}$ at T=300 K.
[a] Spectroscopic assignment of the vibrational band.
[b] Calculated using a fictitious value of $\tilde{\nu}_{fi} = 50.0\,cm^{-1}$ in Eq. (19) in order to estimate S_{vib} for the ground-state rotational spectrum.

$B \approx C$. Consequently, we can view $^{121}SbH_3$ as a quasi-spherical top. The constants B and C are sufficiently large that only states with moderate values of J (up to around 20) are populated at T=300 K, and we can thus generate a converged value of the partition function Q considering this range of J values in the calculation of Q. This is illustrated in Fig. 1. We estimate that in terms of the vibrational basis set (i.e., P_{max}=10), Q is converged to better than 0.1%.

The results of the simulations (line strengths, Einstein coefficients, and absorption intensities) are included in the supporting information along with a Fortran program to generate a synthetic spectrum. As an illustration, we show in Fig. 2 the strongest absorption bands from the chosen wavenumber window. In the same figure the complete spectrum (with wavenumbers from 0 to 8000 cm^{-1}) is also depicted with a logarithmic ordinate scale. The complete SbH_3 list is also available electronically in compressed form at http://www.spectrove.org.

In Table 5 the vibrational transition moments

$$\mu_{fi} = \sqrt{\sum_{\alpha=x,y,z} |\langle \Psi^{\Gamma_f}_{J=0,f} | \overline{\mu}_\alpha | \Psi^{\Gamma_i}_{J=0,i} \rangle|^2} \quad (18)$$

for a number of selected transition lines are given. In Eq. (18), $\Psi^{\Gamma_w}_{J=0,w}$ (w=i or f) are the vibrational wavefunctions. The electronically averaged dipole moment functions $\overline{\mu}_\alpha$ in Eq. (18) are derived from the *ab initio* dipole moment surface SDB-TZ (Table 4). We have computed the transition moments in Eq. (18) for all vibrational transitions that are relevant for the T=300 K absorption spectrum. The strength of the vibrational band at a given temperature [59,60] is

$$S_{vib}(f \leftarrow i) = \frac{8\pi^3 \tilde{\nu}_{fi}}{3hc} \frac{LT_0}{Q_{vib}(T)T} e^{-E_i/kT} [1 - e^{-(E_f - E_i)/kT}] \mu^2_{fi}, \quad (19)$$

Table 6
Experimental and calculated relative intensities of $^{121}SbH_3$ for transitions from the vibrational ground state to pure stretching states.

State[a]	I_{obs}[b]	I_{Hal}[c]	I_{Liu}[d]	$I_{calc.}$[e]
(100;000;A_1/E)	1.0	1.0	1.0	1.0[f]
(200;000;A_1/E)	0.022	0.021	0.021	0.022[f]
(110;000;A_1)[g]		0.20×10^{-4}		0.15×10^{-4}
(110;000;E)		0.98×10^{-5}		0.11×10^{-3}
(300;000;A_1/E)	0.32×10^{-3}	0.47×10^{-3}	0.20×10^{-3}	0.28×10^{-3}[f]
(210;000;A_1)	0.11×10^{-4}	0.82×10^{-7}	0.11×10^{-5}	0.51×10^{-5}
(210;000;E)[h]		0.79×10^{-7}		0.15×10^{-4}
(210;000;E)[i]				0.1×10^{-10}
(400;000;A_1/E)	0.14×10^{-4}	0.78×10^{-5}	0.28×10^{-5}	0.36×10^{-4}[f]

[a] Spectroscopic local-mode assignment of the vibrational band. The calculated energies are given in Tables 1 and 5 unless otherwise indicated.
[b] Observed relative intensities [35].
[c] Calculated relative intensities [35].
[d] Calculated relative intensities [44].
[e] Relative intensities calculated in the present work from the $S_{vib}(f \leftarrow i)$ values in Table 5.
[f] Obtained by adding the A_1 and E intensities.
[g] Calculated energy is 3777.34 cm^{-1}.
[h] Calculated energy is 5606.10 cm^{-1}.
[i] Calculated energy is 5639.07 cm^{-1}.

where E_i and E_f are the band centers of the initial and final states, respectively, and $hc\tilde{\nu}_{fi} = E_f - E_i$, h is the Planck constant, c is the speed of light in vacuum, k is the Boltzmann constant, $L = 2.68675 \times 10^{19}$ mol cm^{-3} atm^{-1} is the Loschmidt constant for 1 atm pressure at the reference temperature of T_0=273.15 K, and T=300 K. In the calculation of the vibrational strength $S_{vib}(f \leftarrow i)$, Q_{vib}=8.34. In Table 5 we have compiled the transition moments of stibine that correspond to band strengths $S_{vib}(f \leftarrow i) > 0.02$ cm^{-2} atm^{-1}. The complete list of computed transition moments and band strengths is given in the supporting information.

In Table 6 we list relative vibrational intensities for a number of vibrational bands and compare them with the corresponding experimental values from Ref. [35] and with other theoretical values [35,44]. For all transitions with available, experimentally derived intensity values (Table 6), the present work has improved the agreement with experiment significantly relative to the previous calculations [35,44].

5. Local mode analysis: comparison of SbH_3 and PH_3

It is well known that the local-mode character of molecules such as phosphine and stibine manifests itself in their geometries, energy level patterns, potential energy and dipole moment surfaces as well in their transition moments (see, for example, Refs. [24,25] and our recent local mode analysis of PH_3 in Ref. [17]). It is also generally accepted that for molecules with local-mode character, the local-mode quantum numbers represent a more adequate labeling scheme for the molecular states, especially for the stretching modes. In the case of stibine this has been shown in Refs. [34,35,37,42].

Here, we compare the local-mode characters of phosphine PH_3 and stibine $^{121}SbH_3$. We expect that stibine exhibits a stronger local-mode character than phosphine, due to the very large mass of the central atom in stibine. Besides, the equilibrium interbond angles of $^{121}SbH_3$ are 91.6° [38] and so they are closer to 90° than the corresponding angles of PH_3 which are 93.4° [61]. In Fig. 3 the vibrational stretching energy patterns for stibine and phosphine are compared up to the polyad 4, where the pure stretching term values are plotted relative to the lowest state in each polyad and labeled according to the local-mode scheme. The theoretical PH_3 energies are taken from Ref. [17], while the stibine energies are from the present work.

The local mode effects become stronger with increasing stretching excitation. This is visible in Fig. 3, where the local-mode degeneracies (for example, of the lowest two levels in each polyad) generally get more pronounced as the polyad number increases. The lowest energy in the polyad has the local-mode label (n,0,0); it is the 'most local' level in the polyad. The higher energies in the polyad correspond to states with a higher degree of mixing between local-mode basis states; these states are less local. However, this energy pattern can be perturbed by the presence of bending levels, especially in the high

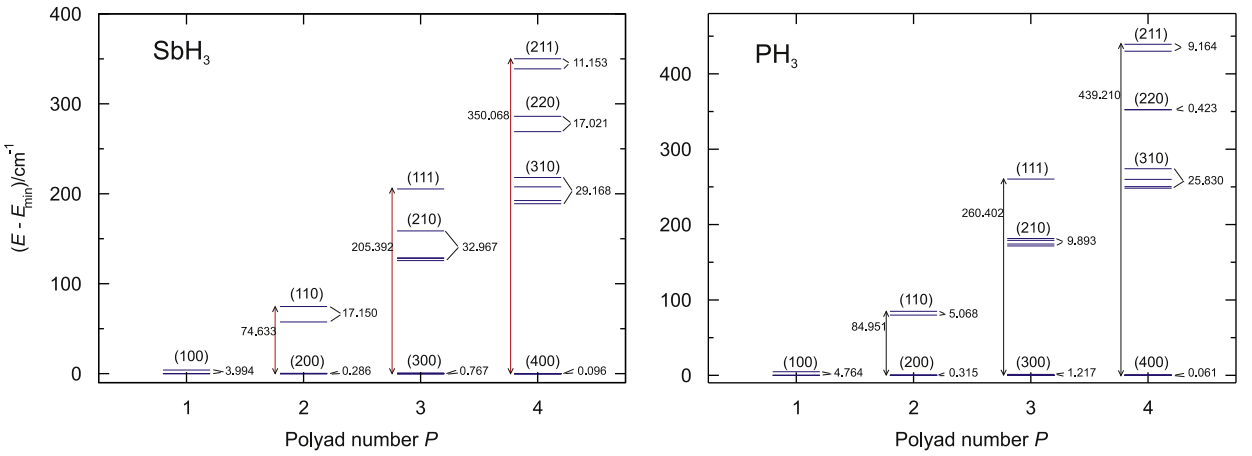

Fig. 3. Comparison between the term value diagrams for the $P \leq 4$ vibrational polyads of PH_3 and $^{121}SbH_3$. The term values (in cm^{-1}) are plotted relative to the lowest state in each polyad. The stretching states are labeled by the local-mode labels (n_1, n_2, n_3).

energy regions with a high density of states. For more details see, for example, the review [25]. Comparing the energy differences of (n,0,0) states in the local mode diagrams of stibine and phosphine in Fig. 3, stibine shows a more pronounced local mode character than phosphine. We also note that in stibine, the stretching vibrations are more harmonic than in phosphine. This is manifest in the smaller energy spread of each polyad.

It was shown in Ref. [17] that according to local-mode theory, the vibrational transition moments for the pure stretching states obey the following simple rule:

$$|\langle n00; E|\boldsymbol{\mu}|000; A_1\rangle| = 2|\langle n00; A_1|\boldsymbol{\mu}|000; A_1\rangle|, \tag{20}$$

where n is the stretching local quantum number and $|\langle n00; \Gamma|\boldsymbol{\mu}|000; \Gamma'\rangle|$ denotes the transition moment μ_{fi} from Eq. (18) between the $|n00; \Gamma\rangle$ and $|000; \Gamma'\rangle$ states. This can be readily verified by inspecting Table 5. For the transition moments μ_{fi} that couple the ground state with the stretching states (100) and (200) we obtain

$$\frac{|\langle 100; E|\boldsymbol{\mu}|000; A_1\rangle|}{2|\langle 100; A_1|\boldsymbol{\mu}|000; A_1\rangle|} = \frac{0.251386}{0.291202} \approx 0.86 \tag{21}$$

and

$$\frac{|\langle 200; E|\boldsymbol{\mu}|000; A_1\rangle|}{2|\langle 200; A_1|\boldsymbol{\mu}|000; A_1\rangle|} = \frac{0.025799}{0.033452} \approx 0.77. \tag{22}$$

That is, Eq. (20) is fairly well satisfied for SbH_3. For PH_3, the corresponding ratios were 0.99 and 0.91 [17], respectively, so that in this case we obtained better agreement with Eq. (20) than for SbH_3.

Finally, in Ref. [17] it was shown that the local mode transition moments $\langle 0|\boldsymbol{\mu}|200; A_1\rangle$ and $\langle 0|\mu|100; A_1\rangle$ satisfy the following condition:

$$\frac{|\langle 0|r|2\rangle|}{|\langle 0|r|1\rangle|} \approx \frac{|\langle 0|\boldsymbol{\mu}|200; A_1\rangle|}{|\langle 0|\boldsymbol{\mu}|100; A_1\rangle|}, \tag{23}$$

where $|\langle 0|r|2\rangle$ is the matrix element of one of the stretching coordinate r_i (i=1,2,3) on the corresponding 1D stretching function represented by the Morse oscillator. For $^{121}SbH_3$ we obtain

$$\frac{|\langle 0|r|2\rangle|}{|\langle 0|r|1\rangle|} \approx 0.09 \quad \text{and} \quad \frac{|\langle 0|\boldsymbol{\mu}|200; A_1\rangle|}{|\langle 0|\boldsymbol{\mu}|100; A_1\rangle|} \approx 0.11, \tag{24}$$

so that the relation in Eq. (23) is better obeyed than in the case of PH_3, where the corresponding quantities were 0.05 and 0.11, respectively.

6. Summary and conclusion

We have reported here a new PES for SbH_3, obtained by empirical refinement of an *ab initio* PES [27], together with a new *ab initio* DMS, computed with the CCSD(T) method as described in Section 4. The new PES and DMS have been used as input for the program TROVE [9] to compute the vibrational energies of $^{121}SbH_3$ up to 8000 cm^{-1} and to simulate the rovibrational spectrum of this molecule in this wavenumber region.

Initially, we calculated the vibrational energies using the high-level *ab initio* PES reported by Canè et al. [27]. The resulting energy values were too large and still far from spectroscopic accuracy. Consequently, an empirical refinement of the PES was performed through a simultaneous fit to the *ab initio* data from Ref. [27] and the available vibrational term values [2]. With the refined PES, we obtained vibrational term values in good agreement with the experimental values. The energies and intensities obtained with the resulting PES and the new DMS were used in a local-mode analysis of $^{121}SbH_3$ whose local-mode behavior was compared to that of phosphine [17].

For stibine, only very limited experimental spectroscopic data is available which do not suffice to determine uniquely the PES in an appreciable volume of configuration space. In particular, there is a paucity of experimentally characterized excited bending levels and levels involving simultaneous excitation of bending and stretching. Therefore, it is impossible to derive a suitable spectroscopic PES purely from experimental data so that a simultaneous fitting to *ab initio* data and the available experimentally derived vibrational energies is inevitable.

In view of the good agreement with the available experimental data obtained with the refined PES and the new *ab initio* DMS, we are confident that we can accurately predict the energies and the intensities of transitions not yet observed, for example those involved in $^{121}SbH_3$ polyads at higher energies as well as the missing bending and bend-stretch levels at lower energies, in particular if we use the CVBS extrapolation method for this purpose [16]. Also, we can make predictions for other isotopologues such as $^{123}SbH_3$, for which there is a dramatic lack of experimental data (see Ref. [27]) and only limited theoretical information [27,35]. We hope that the predictions of the present work will encourage new experimental investigations of $^{121}SbH_3$ and its isotopologues.

Acknowledgments

We acknowledge support from the European Commission through Contract no. MRTN-CT-2004-512202 'Quantitative Spectroscopy for Atmospheric and Astrophysical Research' (QUASAAR). The work of P.J. is supported in part by the Fonds der Chemischen Industrie and that of M.C. by the Andalusian Government (Spain) under the project Contract number P07-FQM-03014.

Appendix A. Supplementary data

Supplementary data associated with this article can be found in the online version at doi:10.1016/j.jqsrt.2010.03.008.

References

[1] Lin H, Thiel W, Yurchenko SN, Carvajal M, Jensen P. J Chem Phys 2002;117:11265–76.
[2] Yurchenko SN, Carvajal M, Jensen P, Herregodts F, Huet TR. Chem Phys 2003;290:59–67.
[3] Yurchenko SN, Carvajal M, Jensen P, Lin H, Zheng JJ, Thiel W. Mol Phys 2005;103:359–78.
[4] Yurchenko SN, Carvajal M, Thiel W, Lin H, Jensen P. Adv Quant Chem 2005;48:209–38.
[5] Yurchenko SN, Carvajal M, Lin H, Zheng JJ, Thiel W, Jensen P. J Chem Phys 2005;122:104317 [14pp.].
[6] Yurchenko SN, Carvajal M, Thiel W, Jensen P. J Mol Spectrosc 2006;239:71–87.
[7] Yurchenko SN, Thiel W, Carvajal M, Jensen P. Chem Phys 2008;346:146–59.
[8] Hougen JT, Bunker PR, Johns JWC. J Mol Spectrosc 1970;34:136–72.
[9] Yurchenko SN, Thiel W, Jensen P. J Mol Spectrosc 2007;245:126–40.
[10] Yurchenko SN, Barber RJ, Yachmenev A, Thiel W, Jensen P, Tennyson J. J Phys Chem A 2009;113:11845–55.
[11] Papoušek D, Aliev MR. Molecular vibrational–rotational spectra. Amsterdam: Elsevier; 1982.
[12] Yurchenko SN, Thiel W, Patchkovskii S, Jensen P. Phys Chem Chem Phys 2005;7:573–82.
[13] Yurchenko SN, Zheng J, Lin H, Jensen P, Thiel W. J Chem Phys 2005;123:134308 [14pp.].
[14] Yurchenko SN, Breidung J, Thiel W. Theor Chem Acc 2005;114: 333–40.
[15] Yurchenko SN, Thiel W, Jensen P. J Mol Spectr 2006;240:174–87.
[16] Ovsyannikov RI, Thiel W, Yurchenko SN, Carvajal M, Jensen P. J Chem Phys 2008;129:044309 [8pp.].
[17] Ovsyannikov RI, Thiel W, Yurchenko SN, Carvajal M, Jensen P. J Mol Spectrosc 2008;252:121–8.
[18] Ovsyannikov RI, Melnikov VV, Thiel W, Jensen P, Baum O, Giesen TF, et al. J Chem Phys 2008;129:044309 [8pp.].
[19] Yurchenko SN, Yachmenev A, Thiel W, Baum O, Giesen TF, Melnikov VV, et al. J Mol Spectrosc 2009;257:57–65.
[20] Yachmenev A, Yurchenko SN, Jensen P, Melnikov VV, Baum O, Giesen TF, et al. to be published.
[21] Yurchenko S, Ovsyannikov RI, Thiel W, Jensen P. J Mol Spectrosc 2009;256:119–27.
[22] Burgdorf MJ, Orton GS, Encrenaz T, Davis GR, Lellouch E, Sidher SD, et al. Adv Space Res 2004;34:2247–50.
[23] Agúndez M, Cernicharo J, Pardo JR, Guélin M, Phillips TG. Astron Astrophys 2008;485:33–6.
[24] Child MS, Halonen L. Adv Chem Phys 1984;57:1–57.
[25] Jensen P. Mol Phys 2000;98:1253–85.
[26] Breidung J, Thiel W. J Mol Spectrosc 1995;169:166–80.
[27] Canè E, Di Lonardo G, Fusina L, Jerzembeck W, Bürger H, Breidung J, et al. Mol Phys 2005;103:557–77.
[28] Bergner A, Dolg M, Küchle W, Stoll H, Preuss H. Mol Phys 1993;80:1431–41.
[29] Martin J, Sundermann A. J Chem Phys 2001;114:3408–20.
[30] Kendall RA, Dunning TH, Harrison RJ. J Chem Phys 1992;96:6796–806.
[31] Loomis CC, Strandberg MWP. Phys Rev 1951;81:798–807.
[32] Jache AW, Blevins GS, Gordy W. Phys Rev 1955;97:680–3.
[33] Helminger P, Beeson Jr. EL, Gordy W. Phys Rev A 1971;3:122–6.
[34] Halonen M, Halonen L, Bürger H, Moritz P. J Chem Phys 1991;95:7099–107.
[35] Halonen M, Halonen L, Bürger H, Moritz P. J Phys Chem 1992;96:4225–31.
[36] Dinelli BM, Corbelli G, Fantoni AC, Scappini F, Di Lonardo G, Fusina L. J Mol Spectrosc 1992;153:307–15.
[37] Lummila J, Lukka T, Halonen L, Bürger H, Polanz O. J Chem Phys 1996;104:488–98.
[38] Fusina L, Di Lonardo G, De Natale P. J Chem Phys 1998;109:997–1003.
[39] Harder H, Gerke C, Fusina L. J Chem Phys 2001;114:3508–23.
[40] Fusina L, Di Lonardo G. J Mol Spectrosc 2002;216:493–500.
[41] Amezcua-Eccius CA, Álvarez-Bajo O, Sánchez-Castellanos M, Lemus R. J Mol Spectrosc 2006;240:164–73.
[42] Sánchez-Castellanos M, Amezcua-Eccius CA, Álvarez-Bajo O, Lemus R. J Mol Spectrosc 2008;247:140–59.
[43] Pluchart L, Leroy C, Sanzharov N, Michelot F, Bekhtereva E, Ulenikov O. J Mol Spectrosc 2005;232:119–36.
[44] Liu A-W, Hu S-M, Ding Y, Zhu Q-S. Chin Phys 2005;14:1946–53.
[45] Bunker PR, Jensen P. Molecular symmetry and spectroscopy, second ed.. Ottawa: NRC Research Press; 1998.
[46] Numerov B. Mon Not R Astron Soc 1924;84:592–602.
[47] Cooley JW. Math Comput 1961;15:363–74.
[48] Bunker PR, Landsberg BM. J Mol Spectrosc 1977;67:374–85.
[49] Wilson EB, Decius JC, Cross PC. Molecular vibrations. New York: McGraw-Hill; 1955.
[50] Mátyus E, Czakó G, Császár AG. J Chem Phys 2009;130:134112.
[51] Yurchenko SN, Zheng JJ, Lin H, Jensen P, Thiel W. J Chem Phys 2005;123:134308.
[52] Purvis GD, Bartlett RJ. J Chem Phys 1982;76:1910–8.
[53] Raghavachari K, Trucks GW, Pople JA, Head-Gordon M. Chem Phys Lett 1989;157:479–83.
[54] Werner HJ, Knowles PJ, Bernhardsson A, Berning A, et al., with contributions from Amos RD, MOLPRO, version 2002.3 and 2002.6, a package of *ab initio* programs; 2002.
[55] Hampel C, Peterson K, Werner HJ. Chem Phys Lett 1992;190:1–12.
[56] Wood J, Boring A. Phys Rev B 1978;18:2701–11.
[57] Mecke R. Z Electrochem 1950;54:38–42.
[58] Marquardt R, Quack M, Thanopulos I, Luckhaus D. J Chem Phys 2003;119:10724–32.
[59] Zare RN. Angular momentum. New York: Wiley; 1988 [section 6.5].
[60] Cottaz C, Tarrago G, Kleiner I, Brown LR. J Mol Spectrosc 2001;209:30–49.
[61] Kijima K, Tanaka T. J Mol Spectrosc 1981;89:62–75.